Reconfigurable All-Optical Integrated Nonlinear Activator with Switchable Response Functions for Photonic Neural Networks

Bei Chen,[1,*] Jian Wang,[1] Zichao Zhao,[2] Xiaowen Xiong,[3] Jianyi Yang,[2] Ming Li,[1] and Ninghua Zhu[1,4]

[1] *State Key Laboratory on Integrated Optoelectronics, Institute of Semiconductors, Chinese Academy of Sciences, Beijing 100083, China*
[2] *College of Information Science and Electronic Engineering, Zhejiang University, Hangzhou 310027, China*
[3] *Department of Electronic Engineering, Tsinghua University, Beijing 100084, China*
[4] *Communication and Integrated Photonics Laboratory, Xiongan Institute of Innovation, Chinese Academy of Sciences, Xiongan New Area 071899, China*

[*] *beichen@semi.ac.cn*

Abstract: We experimentally demonstrate a reconfigurable all-optical integrated nonlinear activator with switchable response functions, including Gaussian, Radial Basis, Softplus, leaky ReLU, Swish and clamped ReLU functions, especially all triggered by low-power inputs.

1. Introduction

The rapid development of photonic neural networks (PNNs) primarily rests on the high-speed parallel computing capability, high energy efficiency and low latency of photonics, compared to the existing electronic architectures. In recent years, optical linear matrix-vector multiplication (MVM) as a fundamental unit of PNNs have been realized by multiple methods, including free-space light conversion [1], cascaded Mach-Zehnder interferometer (MZI) topology [2] and wavelength division multiplexing (WDM)-based architecture [3]. It is worth noting that an algorithm of artificial neural network (ANN) only consisting of linear layers can not deal with complex issues. Only combined with nonlinear activators, the corresponding algorithm can realize a higher dimensional computing, so as to figure out complex mapping relationships in various scenarios. Hence, optical nonlinear activator (ONA) as another basic unit in PNNs is indispensable. To date, ONAs based on electro-optic hardware [4–6] or all-optical platform [7–9] have been proposed. However, most of them can not satisfy all requirements of a practical ONA, such as low threshold of input power, multiple switchable response functions, large operating bandwidth, without electronic assistance or optical-electrical-optical conversion, on-chip integration and compact footprint.

In this work, we experimentally demonstrate a reconfigurable all-optical ONA by using the Fano-enhanced MZI-embedded microring resonator (MZER) structure based on integrated silicon-on-insulator (SOI) platform, where Fano effect would enhance the optical nonlinearity in SOI including free-carrier dispersion (FCD) and Kerr effect. Utilizing multiple programmable thermal-optical (TO) phase shifters in the Fano-enhanced MZER and the cavity intensity buildup, various switchable nonlinear response functions with tunable thresholds and slope rates

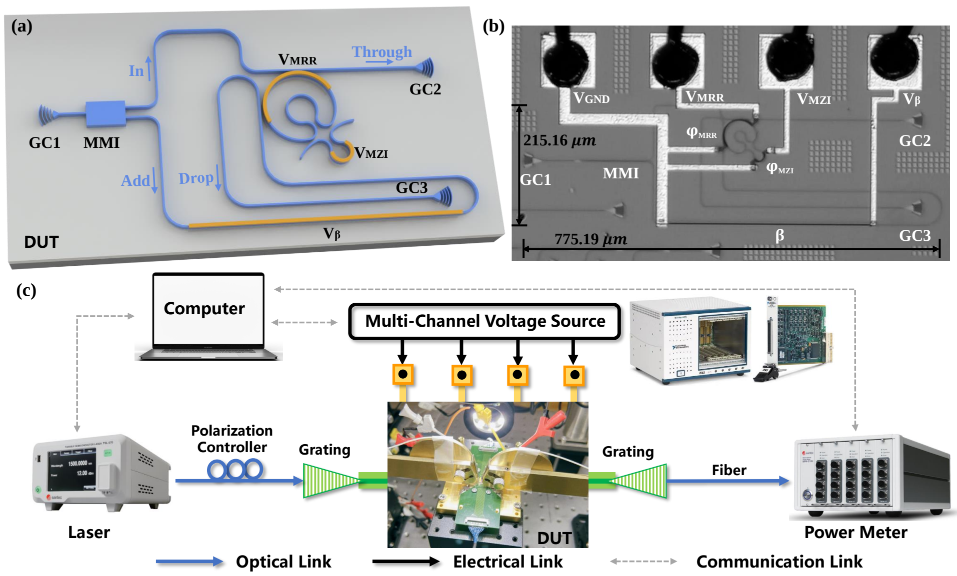

Fig. 1. (a) Reconfigurable all-optical integrated nonlinear activator based on Fano-enhanced MZER structure. (b) Microscope view. (c) Illustration of the experimental setup.

can be realized, including Gaussian, Radial Basis, Softplus, leaky ReLU, Swish and clamped ReLU functions. Our proposed device might provide another solution of the ONA with low threshold, compact footprint, switchable and tunable response functions for large-scale integrated PNNs.

2. Device Fabrication

The proposed Fano-enhanced MZER structure, as depicted in Fig. 1(a), is composed of a 1×2 multimode interference (MMI) and an add/drop microring resonator (MRR) embedded with a symmetric MZI. Light is coupled into the structure by the input grating coupler (GC), and split into two branches with equal power by the 1×2 MMI. The upper branch can be seen as the ”In” port of the add/drop MRR, and the corresponding lower one is the ”Add” port. Along the Add port, an additional TO phase shifter is introduced to provide a tunable phase variance ”β” between In port and Add port. Triggered by these two branches with asymmetric phases, Fano resonance [10] is occurred in the MZER. In addition, the MZER cavity buildup triggers FCD and Kerr effect, which manifest as a nonlinear phase response to optical power. Correspondingly, the nonlinear phase is converted to nonlinear transmission via the embedded MZI. The reconfigurability of the Fano-enhanced MZER structure is realized by TO phase shifters on the MRR, the embedded MZI and the waveguide along Add port. These together generate various nonlinear response functions with switchable function types, tunable thresholds and programmable slope rates.

The device is fabricated on an 8-inch SOI wafer with 220-nm-thick silicon layer and 2-μm thick buried oxide layer by Advanced Micro Foundry (AMF). Fig. 1(b) shows its microscope image. The footprint including GCs and Fano-enhanced MZER is about 775.19 μm×215.16 μm, which can be further minimized by layout optimization. The radius of the add/drop MRR is set as 30 μm. Besides, the radius of inner curved waveguide and the length of the embedded-MZI arm are set as 10 μm and 94.25 μm, respectively. Additionally, the coupling efficiency between the curved waveguides is designed to be 50:50, and the gap of evanescent coupling region is 240 nm. GCs are used for fiber coupling and to support the fundamental quasi-transverse electric (TE) mode. In further, the pads on the optical chip are bonded to the printed circuit board for further tuning.

3. Experimental Results

The experimental setup of the proposed Fano-enhanced MZER structure used as an ONA is shown in Fig. 1(c). The injected continuous light is generated by a single-mode laser (Santec TSL-570). The light transmitted through the device is detected by using an optical power meter (Santec MPM-210). Moreover, the applied voltages on three TO heaters are provided by the analog output module (NI PXI-6704). The input laser, optical power meter and multi-channel voltage source are all controlled by a computer, which also simultaneously records the input and output powers of the tested device.

To achieve the transfer functions representing the instantaneous input and output powers, a three-dimensional sweep of the applied voltages is generated and applied to the TO heaters, automatically controlled by the self-defined scripts on Matlab platform. Figs. 2(a)-2(f) depict various switchable nonlinear activation functions with tunable thresholds and slope rates under different applied voltages, including Gaussian, Radial Basis, Softplus, leaky ReLU, Swish and clamped ReLU functions. The input power of the Fano-enhanced MZER structure lies in the range of 0 to 6.3 mW. Correspondingly, the output powers are varied within different ranges, depending

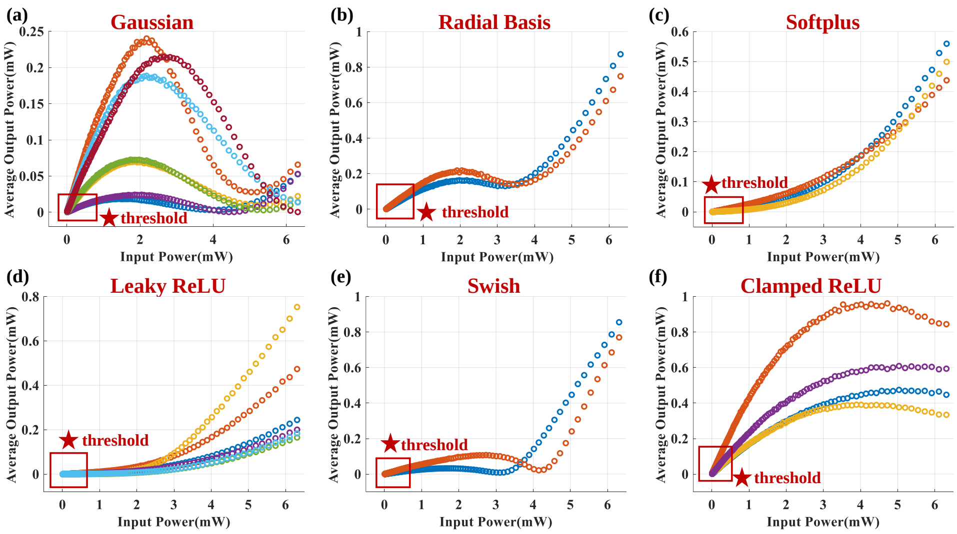

Fig. 2. Experimental results of six switchable nonlinear functions, including (a) Gaussian, (b) Radial Basis, (c) Softplus, (d) leaky ReLU, (e) Swish and (f) clamped ReLU functions.

(a)
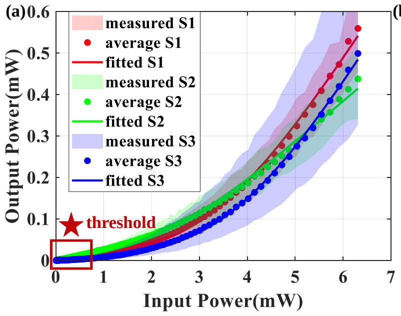

(b)

Parameter	Softplus (S1)	Softplus (S2)	Softplus (S3)
a	0.1796	0.09984	0.1853
b	0.9795	0.9172	0.9804
x_0	3.343	2.173	3.769
R^2	0.9981	0.9968	0.9991
RMSE	0.004234	0.004713	0.002458

$$f(x) = a \cdot \ln(b + e^{x-x_0})$$

Fig. 3. (a) The measured response functions ”Softplus” with reconfigurable parameters, including the corresponding average results and fitted results. (b) Corresponding parameter list.

on different types of the transfer activation functions. It is worth noting that the input and output powers of the device are both maintained under the absolute measured values without any normalization. The reason is that once we use any method of normalization, the shapes of response functions would be changed, respective to the slope rates and other detailed parameters in mathematical expressions. Moreover, one type of activation function with different parameters would have different performances in ANN algorithms, which means that these detailed changes should be kept for further performance tests of ANNs. Besides, it can be seen that all measured nonlinear activation functions are triggered with low-power inputs. As a specific example, Figs. 3(a) and 3(b) show the measured activation functions ”Softplus” with reconfigurable parameters. Each measured transfer curve is tested by five times under the same experimental parameters, which indicates that the proposed device has inevitable measured error due to the cavity carrier lifetime and the thermal dissipation. Besides, the dotted curves are the average results of the five-time experimental values. Furthermore, we use the expression in type of $f(x) = a \cdot ln(b + e^{x-x_0})$ to derive the fitted results. As a result, the limited values of root-mean-square error (RMSE), used as the evaluation criteria, validate their good performances and the feasibility of the fitted function type.

4. Conclusion

A reconfigurable all-optical ONA based on silicon-integrated Fano-enhanced MZER structure is proposed and experimentally demonstrated. Such a device can realize various switchable nonlinear response functions with low thresholds and tunable slope rates, including Gaussian, Radial Basis, Softplus, leaky ReLU, Swish and clamped ReLU functions. Future work will be devoted to enlarging the operating bandwidth and applying the device to various scenarios.

Acknowledgements

This research is supported by the National Natural Science Foundation of China under Grant 62235011 and 62075212, the China Postdoctoral Science Foundation under Grant BX20230172 and 2023M731884.

References

1. X. Lin, Y. Rivenson, N. T. Yardimci, M. Veli, Y. Luo, M. Jarrahi, and A. Ozcan, “All-optical machine learning using diffractive deep neural networks,” Science **361**, 1004–1008 (2018).
2. Y. Shen, N. C. Harris, S. Skirlo, M. Prabhu, T. Baehr-Jones, M. Hochberg, X. Sun, S. Zhao, H. Larochelle, D. Englund *et al.*, “Deep learning with coherent nanophotonic circuits,” Nat. photonics **11**, 441–446 (2017).
3. A. N. Tait, T. F. De Lima, E. Zhou, A. X. Wu, M. A. Nahmias, B. J. Shastri, and P. R. Prucnal, “Neuromorphic photonic networks using silicon photonic weight banks,” Sci. reports **7**, 7430 (2017).
4. I. A. Williamson, T. W. Hughes, M. Minkov, B. Bartlett, S. Pai, and S. Fan, “Reprogrammable electro-optic nonlinear activation functions for optical neural networks,” IEEE J. Sel. Top. Quantum Electron. **26**, 1–12 (2019).
5. J. R. R. Campo and D. Pérez-López, “Reconfigurable activation functions in integrated optical neural networks,” IEEE J. Sel. Top. Quantum Electron. **28**, 1–13 (2022).
6. C. Pappas, S. Kovaios, M. Moralis-Pegios, A. Tsakyridis, G. Giamougiannis, M. Kirtas, J. Van Kerrebrouck, G. Coudyzer, X. Yin, N. Passalis *et al.*, “Programmable tanh-, elu-, sigmoid-, and sin-based nonlinear activation functions for neuromorphic photonics,” IEEE J. Sel. Top. Quantum Electron. (2023).
7. A. Jha, C. Huang, and P. R. Prucnal, “Reconfigurable all-optical nonlinear activation functions for neuromorphic photonics,” Opt. letters **45**, 4819–4822 (2020).
8. Y. Shi, J. Ren, G. Chen, W. Liu, C. Jin, X. Guo, Y. Yu, and X. Zhang, “Nonlinear germanium-silicon photodiode for activation and monitoring in photonic neuromorphic networks,” Nat. Commun. **13**, 6048 (2022).
9. B. Wu, H. Li, W. Tong, J. Dong, and X. Zhang, “Low-threshold all-optical nonlinear activation function based on a ge/si hybrid structure in a microring resonator,” Opt. Mater. Express **12**, 970–980 (2022).
10. U. Fano, “Effects of configuration interaction on intensities and phase shifts,” Phys. review **124**, 1866 (1961).